HETEROSTRUCTURE BARRIER MIXERS FOR TERAHERTZ APPLICATIONS

F. Podevin, P. Mounaix, O. Vanbésien, M. Chaubet * and D. Lippens

Institut d'Electronique et de Microélectronique du Nord, UMR 8520
Université des Sciences et Technologies de Lille
Avenue Poincaré, BP 69, 59652 Villeneuve d'Ascq Cedex, France
* Centre National d'Etudes Spatiales
18 Avenue Edouard Belin,31401 Toulouse Cedex, France
Corresponding author: Florence.Podevin@IEMN.univ-Lille1.fr

Abstract : This paper deals with Schottky - and Heterostructure - Barrier devices fabricated for planar integration in a 560 GHz Subharmonic Mixer (SHM). Taking advantage of an InP-based technology, two barrier types, metal/InGaAs and metal/InAlAs/InGaAs respectively, have been investigated. The design was carried out by means of self-consistent quantum calculations and the fabrication involved submicron T-shaped contacts and air-bridge technology for back-to-back integrated diode pairs. The trade-offs between the key figures of merit for SHM are discussed and compared to experimental results. In addition, various studies of the potential of a Planar Doped Heterostructure Barrier for single SHM devices are presented.

Indexing terms *: Heterostructure devices, Subharmonic Mixer, InP technology, Terahertz, Space applications*

1. Introduction

Recently, impressive results have been published about sub-mm subharmonic mixing, notably by the Jet Propulsion Laboratory (JPL) at 560 GHz [1], 640 GHz [2] and 2.5THz [3]. For these demonstrations, a GaAs technology was used with a barrier effect achieved through a metal/GaAs n-doped epilayer junction. The built-in potential (0.7 eV) is adequate for low saturation current, but, as a consequence, the local oscillator power to optimally pump the back-to-back diode pair is relatively high. In addition, the optimization of the series resistance, which is known as one of the key figure of merit for high performance, faces some limits owing to the relatively wide band gap of GaAs (1.4 eV). From this point of view, an InGaAs layer lattice-matched to InP having a narrower gap (E_g

= 0.75 eV) appears to be a better candidate [4]. The ideality factor of InGaAs to metal junctions ranges from ~1.2 to 1.6 (depending on the contact deposition)[5]

However, some drawbacks associated with its low Schottky built-in potential (0. 22 eV) could be pointed out, motivating the use of InAlAs/InGaAs epilayers. In this communication, the trade-offs related to the use of a metal/narrow-gap configuration are firstly addressed to the fabrication on the submicron scale of anti-parallel Schottky diodes and secondly followed by theoretical quantum calculations. In a second stage, we investigate a metal/wide gap/narrow-gap configuration, with theoretical and experimental comparisons. Finally, we deal with the potential of a single Heterostructure Barrier set in conduction mode via δ-doping.

2. Metal/n-type InGaAs contact

From a technological point of view, the active epilayers were grown by a Gas Source MBE on an InP, Fe-doped, substrate. The ohmic contact layer was doped up to $1x10^{19}$ cm^{-3}, whereas the Schottky layer is n-doped with a donor concentration of $2x10^{17}$ cm^{-3}. The anti-parallel diode pair is fully planar. Firstly wet chemical etching was used to perform a recess down to the n^+-doped layer with a trench formation before evaporating the ohmic contact. Subsequently, a one step molding stage was conducted and followed by the metallization of both the Schottky contacts on the submicron scale (gate length down to 0.1 μm) and the free standing air-bridges interconnecting the anodes to the pads. Towards this goal, e-beam molds have been fabricated with a bi-layer electron resist (PMMA/copolymer) via an e-beam patterning at various doses. A SEM view of a typical device, interconnected with 15 μm long tapered air bridges, is shown in Figure 1.

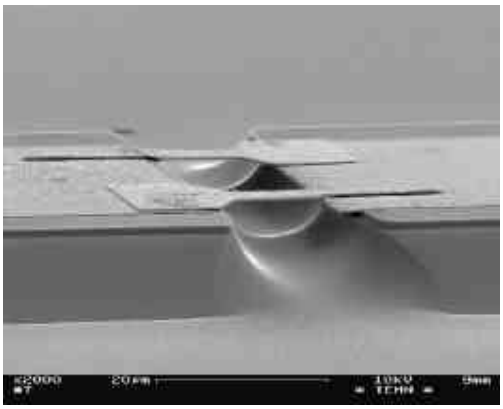

Figure 1 SEM view of a typical diode pair with T-gate 0.1x10 μm² finger shaped Schottky anodes.

On the basis of the previous discussion, the metal/InGaAs devices were developed for low driven power devices. The epilayer design was first conducted by extending, to the Schottky diode case, the in-house code developed earlier for quantum-sized devices [6]. This code was performed in order to solve, in a first stage, the one dimensional Poisson equation when voltages are applied to a given structure (Schottky contact, heterostructure Schottky contact, single barrier varactor, resonant tunneling diodes…). In a second stage, a numerical solution of the Schrödinger equation gives the wave function from which any information concerning the transmission or reflection coefficients is obtained. As shown in the following equation (Eq1), the integral of current density is calculated from the product between the previous transmission and the supply function, on the entire energy continuum :

$$J = \int_0^{+\infty} T(E) \times F(E)\ dE \qquad \text{(Eq1)}$$

Very shortly, one can see in Figure 2, the conduction band bending at zero bias and at 0.3 V for an InGaAs epilayer. When a voltage is applied, the current flows from the semi-conductor to the metal, which is represented on the schematic by the integral of current "through" the potential curve at 0.3V, in arbitrary units. It is very important to take into account all the conduction current contributions (as tunneling field emission for example) to describe in a realistic way the I-V characteristics of narrow gap materials. As a current manner, we do not observe pure tunneling effect (as it would be the case with high gap materials) and the electronic flow is maximal for quasi thermal energy levels, which explains relatively good values for the ideality factor (n is ~1.3).

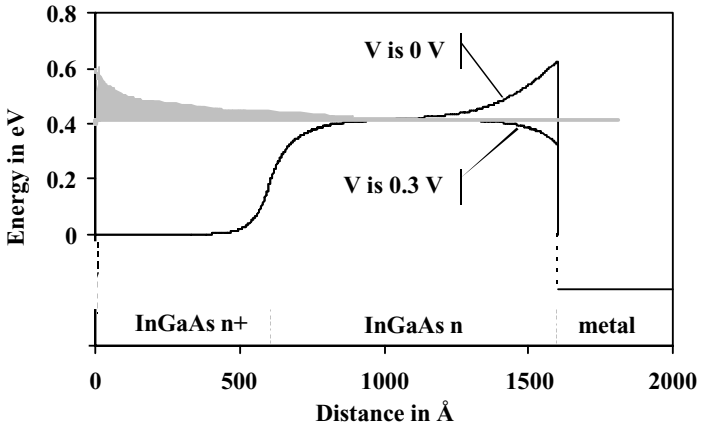

Figure 2 Conduction Band Bending at zero bias and at 0.3Volt.
The InGaAs lattice-matched to InP structure is affected by the applied voltage (0.3V) and thus the current can flow from the semi-conductor to the metal.
The integral of current is also plotted in an arbitrary unit.

Figure 3 shows a comparison between measured and calculated I-V curves, at room temperature. Good agreement is thus obtained between theory and measurement with, as expected, a threshold voltage for conduction onset quite low (V_{bi} ~ 0.15V), and correct ideality factors for InP-based devices.

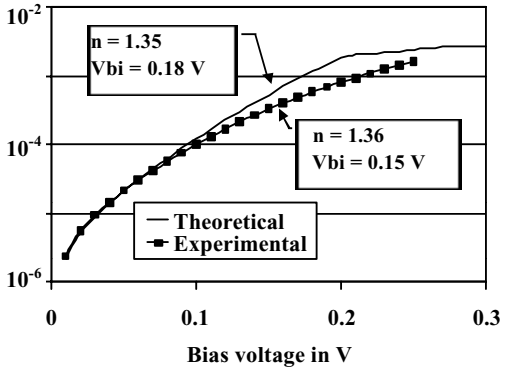

Figure 3 : Comparison between experimental and calculated I-V characteristics for a metal/InGaAs ($2x10^{17}$ cm^{-3}) Schottky contact fabricated in our laboratory.

In order to investigate the influence of such low values of V_{bi} on the mixer performances, some simulations were performed by means of Microwave Design System, by Hewlett Packard. They showed that a strong dependence exists between the mixer performances at 560 GHz and the Schottky diodes electrical characteristics: built-in voltage V_{bi} and ideality factor n (see Figure 4).

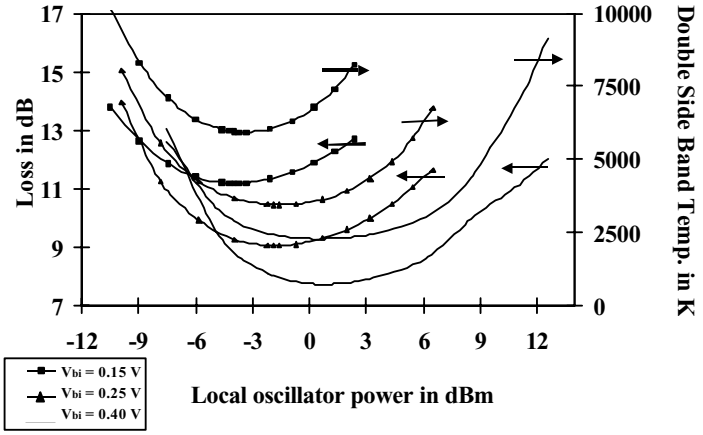

Figure 4 Mixer performances vs the local oscillator power across the diodes. Parameter is the built-in voltage V_{bi}.

As plotted in Figure 4, increasing V_{bi} could afford less loss (L) and smaller double-side-band noise temperature (T_{DSB}). Ideally, L and T_{DSB} are about 8 dB and 2500 K

respectively for a pump power of 1 dBm. This can be explained from the well-established thermal relationship (Eq2) between V_{bi} and I_s, the saturation current :

$$I_s = S_A \cdot T^2 \cdot A^{**} \cdot \exp(-qV_{bi} / k_B T) \qquad \text{(Eq2)}$$

where S_A is the area, T the temperature in K and A** the Richardson constant for InAlAs. This relation shows that increasing V_{bi} decreases I_s, which is known as a source of degradation in terms of mixing performances. Thus, efforts were pointed out towards an heterostructure Schottky diode. By means of an InAlAs layer (Eg is 1.47 eV) we could raise the knee voltage up to about 0.5 V.

3. Metal/InAlAs/InGaAs Schottky contact

As seen previously, the metal/InAlAs/InGaAs junction was fabricated in order to limit the saturation current, which is known as a source of degradation in mixer performances. For all the structures, the InAlAs layer was undoped (doping influence is totally negligible, see Figure 5). Varying its thickness permits us to modulate the conduction properties. Basically the total conduction current is the result of three contributions : (i) pure tunneling from the highly populated states below the Fermi level, (ii) thermally assisted tunneling phenomena and (iii) thermionic emission over the InAlAs barrier. Quantum calculation does not need to make a distinction between these contributions and can be used to investigate the influence of the InAlAs layer. Figure 5 illustrates some of the results showing the thickness dependence of the apparent ideality factor *. There clearly exists an optimum between an ultra thin barrier where pure tunneling current is dominant and a thick barrier where Fowler-Nordheim field emission becomes the significant component. For comparison, we also reported the ideality factors measured for various devices.

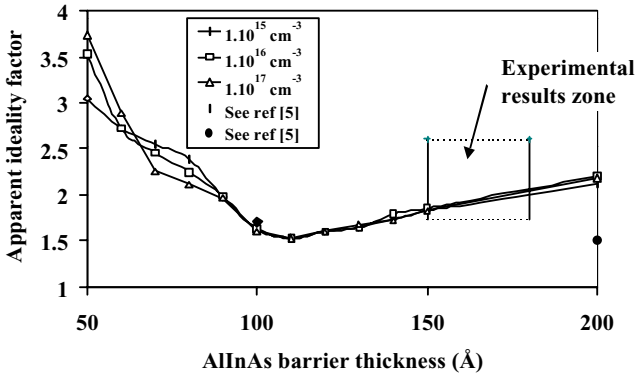

Figure 5 Thickness dependence of the apparent ideality factor in a metal/InAlAs/InGaAs contact layer. Parameter is the InAlAs doping level. Some experimental results are also presented. Dots refer to [5] : ideality factor for an InAlAs barrier thickness of 100Å and 200Å.

* Strictly speaking, the ideality factor is defined for thermionic emission processes. This explains the fact that we used an apparent figure.

As a general rule, the insertion of an InAlAs layer, which was found beneficial for voltage handling, has in counterpart degraded the non-linearity of the diode through an increase of the ideality factor up to 1.5 (in the best case). This result can be explained by observing the energy levels where conduction operates and by studying the different current components. In fact, two effects are in competition. In the thin barriers case, tunneling emission occurs at a relatively low ground energy level E_{tun} compared to the barrier height ϕ_b. When the barrier is getting thicker, the deep tunnel contribution is lowered for the benefit of thermally assisted tunneling conduction processes at higher energies, closer to a thermionic emission process (where n is quasi ideal), which explains the n improvement. In the same time, thick barriers are strongly affected by the triangular-shaped barrier when a voltage is applied. Then, resonant Fowler-Nordheim current components appear. They consist in preferential conduction paths at well-defined quantum-size energy levels E_{FN1}, …, E_{FNn}, revealed by the well-defined peaks in the energy-current distribution. Both cases of the thin and thick barriers for a given electric field in the InAlAs barrier are represented in Figure 6.

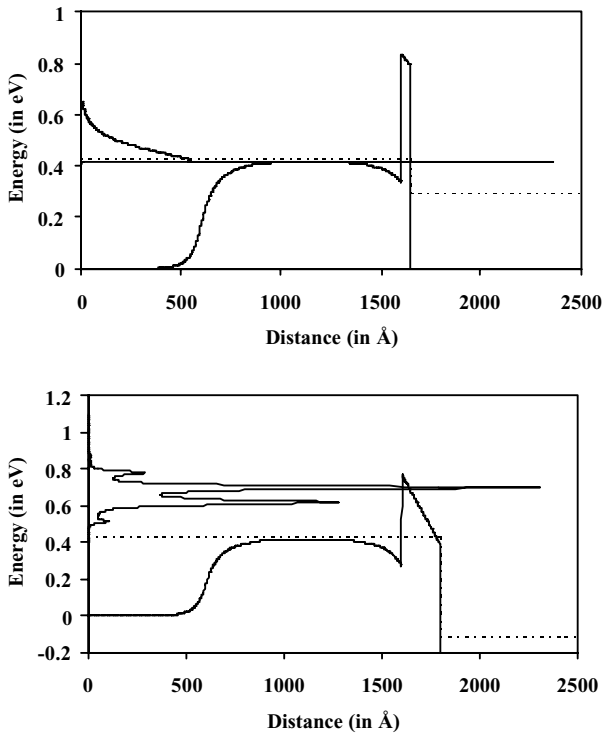

Figure 6 Both figures represent the conduction band bending of a n+-InGaAs / n-InGaAs / InAlAs / metal Schottky heterojunction. The barrier thickness are 50Å and 200Å respectively for the above and below figures. Applied voltages are 0.136V and 0.545V respectively, in order to keep the same electric field in the triangular shape.
In the thin barrier case, conduction is via pure tunneling; in the thick one, four preferential paths are chosen. Doted lines represent the Fermi level in the semi conductor and the metal.

With an increase of the barrier width, the ground quantum level of the resonant Fowler-Nordheim conduction mode tends to bury in the triangular well formed under bias at the wide-gap semiconductor / metal heterointerface, degrading, as a consequence, the ideality factor. Competition between both opposite behaviors (tunneling and Fowler-Nordheim) implies an optimum, reached for a barrier thickness of about 100Å.

4. δ-InGaAs / InAlAs / δ-InGaAs layer

In contrast to the above case, we employed, here, a technology without any Schottky effect. The rectifying barrier is introduced via a Semiconductor Heterostructure Barrier. This gives to the I-V curve, a natural anti-symmetry, in forward and reverse bias conditions. Thus, a Sub Harmonic Mixer could be fabricated by means of a single device, avoiding the parasitic elements inherent to the counter-balanced configuration. Such advantages with a natural anti-symmetry were already exploited for the Heterostructure Barrier Varactors, and hence, for a reactance non-linearity. On this basis, we recently reported the highest performances for a HBV tripler using an InP technology [7].

In the present work, we are taking advantage of the symmetry in a conductive mode. To this end, we designed and fabricated Heterostructure Barrier devices with δ-doping grown plane on each side of the barrier (δ−HB). The epitaxial sequence is shown in Figure 7 (left side). The δ-planes are typically 15Å thick. Practically, their doping concentration can range from $1x10^{12}$ cm^{-2} up to $1x10^{13}$ cm^{-2}. The structure barrier level is 0.54eV with InAlAs (the same barrier as the one used in the heterostructure Schottky contact).

InGaAs	n+=5x10^{18} cm^{-3}	350Å
InGaAs	n=1x10^{15} cm^{-3}	40Å
InGaAs	n_s	15Å
InGaAs	n=1x10^{15} cm^{-3}	45Å
InAlAs	n=1x10^{15} cm^{-3}	h
InGaAs	n=1x10^{15} cm^{-3}	45Å
InGaAs	n_s	15Å
InGaAs	n=1x10^{15} cm^{-3}	40Å
InGaAs	n+=5x10^{18} cm^{-3}	350Å
InP	Semi insulating	

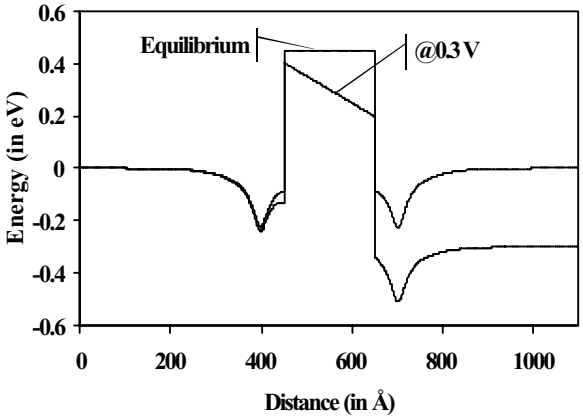

Figure 7 Epitaxial structure of a δ-HB on the left hand side. Potential profile of the same structure at equilibrium and under bias conditions, on the right hand side.
The barrier thickness (h) is 200Å and the sheet doping concentration (n_s) is $1x10^{13}$ cm^{-2}.

In Figure 7 (right hand side), one can see the potential profile of such a symmetric heterostructure, at equilibrium and under bias control. The offset between the Fermi levels on each side of the barrier implies a current flow from higher electronic levels down to lower ones. See [8] for more information on the δ-HB.

If one reminds the parametric study between the "apparent" ideality factor and the barrier thickness performed in the heterostructure Schottky contact case, one can expect a similar dependence in this case. In fact, same effects are observed with an optimum reached for h~100Å. This sounds logical since the triangular barrier well forms identically under bias conditions, and this whatever n_s. However, the optimum is higher with n equal to 2.2. This value is bigger than 2; one reason could be the natural symmetry of the structure, as discussed in [9] for a Planar Doped Barrier (PDB).

Concerning the sheet doping concentration, Figure 8 shows the degree of freedom afforded by n_s variation. It can be shown that the threshold voltage V_{th} depends on the donor concentration, and can be thus modulated practically at will. The δ-doped plane makes the effective barrier height to change. When the planes are highly doped, the wells at each part of the barrier become deeper and the barrier appears to be higher than Φ_b (InAlAs barrier height value). For instance, V_{th} can be as low as 0.2 V for a $1x10^{13}$ cm^{-2} concentration of the δ-planes and as high as 0.8 V for $1x10^{12}$ cm^{-2}.

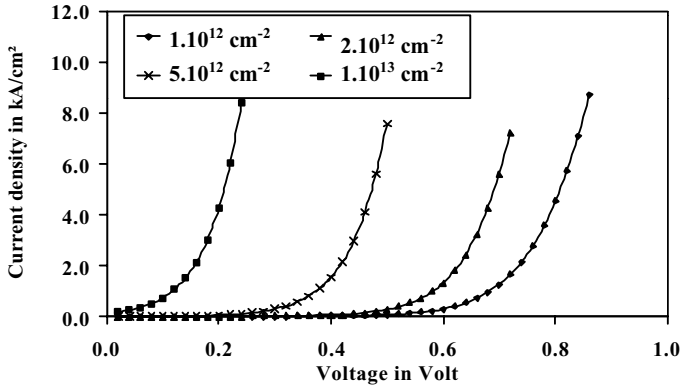

Figure 8 I-V curves at various sheet carrier concentrations in the planar doping.

Experimental study has been realized yet, on a δ-HB with $n_s = 2x10^{12}$ cm^{-2}. The following I-V characteristics (Figure 9) presents a very good asymmetry in the current behavior. The conduction offset is slightly higher than that calculated. This is due to a 30Å AlAs layer that has been incorporated between two InAlAs layers, in order to obtain a symmetric step-like barrier higher than the single InAlAs barrier. See [8].

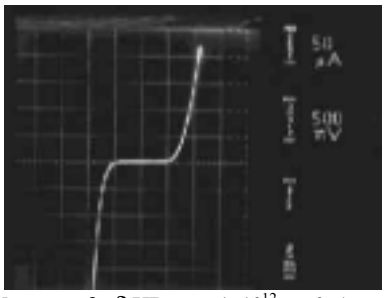

Figure 9 I-V curve of a δ-HB. $n_s = 1x10^{12}$ cm^{-2}. Area = 1256 μm².

5. Conclusion

A compromise can be pointed out between device functionality, technological feasibility, electrical performances and finally compatibility for sub-mm operations. The choice of a specific active layer configuration depends on which features are required for the current framework. Technologically speaking, a knowledge of the pump requirements, loss and noise temperature specifications corresponds to one given component. The large range in the electrical characteristics, which strongly depends on the epitaxial parameters, enables us to chose the most adapted device to the current situation. As an example, the recent advances in solid state sources permits us to relax the pump power in the near future. Concerning the devices design which has been reported here, we aim to use them for applications in the lower part of the Terahertz spectrum. We believe that the advantages of InP could also be exploited at higher frequencies, such as 2.5 THz.

References

[1] Oswald *et al*, IEEE Microwave and Guided Wave Let. Vol 8. P 232. 1998.
[2] Mehdi *et al*, IEEE MTT-S Digest. P 403. 1998.
[3] Siegel *et al*, IEEE Trans. On MTT. Vol 47. P596. 1999.
[4] Kordoš *et al*, J. Appl. Phys. Vol 72. P 2347. 1992.
[5] Marsh *et al*, IEEE Trans. On Electron devices. Vol 45. P 349. 1998.
[6] Burgnies *et al*, JAP. Vol 75. 1 May 1994.
[7] Mélique *et al*, Electronics Let. Vol 35. 27 May 1999.
[8] Lheurette *et al*, IEEE Electron Device Let. Vol 19. No 9. 1998.
[9] Lee *et al*, Microwave and Optical Tech. Let. Vol 4. No 1. P 53. 1993.

This work was supported by CNES contract # 714/98/CNES/7280/00.